

# Experimental Proof of the Non-Least-Motion Cycloadditions of Dichlorocarbene to Alkenes: Kinetic Isotope Effects and Quantum Mechanical Transition States

Amy E. Keating,<sup>†</sup> Steven R. Merrigan,<sup>‡</sup> Daniel A. Singleton,<sup>\*,‡</sup> and K. N. Houk<sup>\*,†</sup>

Contribution from the Department of Chemistry and Biochemistry, University of California, Los Angeles, California 90095-1569, and Department of Chemistry, Texas A&M University, College Station, Texas 77843

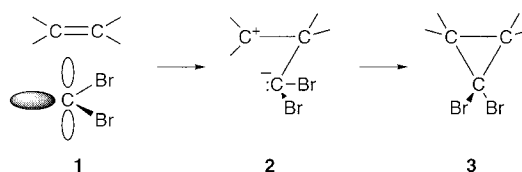
Received April 27, 1998. Revised Manuscript Received February 1, 1999

**Abstract:** High-precision experimental kinetic isotope effects were measured at natural abundance for the cycloaddition of dichlorocarbene to 1-pentene. These values were compared to isotope effects predicted for the addition of dichlorocarbene to propene at the B3LYP/6-31G\* and B3LYP/6-311+G\* levels. The results provide unambiguous evidence for a nonlinear attack in which bond formation is more advanced at the unsubstituted carbon of the terminal alkene in the transition state of the cycloaddition. This is the first experimental confirmation of the unsymmetrical, non-least-motion approach of a carbene to an alkene first proposed by Skell over 40 years ago and predicted by quantum mechanical calculations.

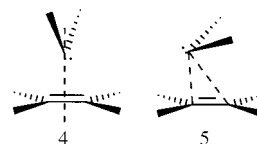
## Introduction

Carbenes undergo cycloadditions to alkenes to form cyclopropanes, and the mechanisms for this reaction have been studied by organic and physical chemists for over 40 years. The stereospecificity of cyclopropanations with dibromocarbene led Skell and Garner in 1956 to postulate simultaneous bonding of singlet carbenes to both olefinic carbons, and the “three-center-type” interaction proposed was interestingly depicted as **1** → **2** → **3**.<sup>1</sup> These structures were the first allusion to a non-least-motion “ $\pi$ -approach” pathway for cyclopropanation, involving initial interaction of the empty p-like orbital of the carbene with the filled  $\pi$  orbital of the alkene. This pathway was first discussed explicitly by Moore et al.<sup>2</sup> and has since been the subject of numerous theoretical studies.<sup>3–9</sup> Experimental evidence for the transition-state geometry has been more difficult to obtain. We report here a combined theoretical/experimental study of isotope effects for cyclopropanations with dichlorocarbene which provides an experimental basis for the non-least-motion pathway for cyclopropanations.

The early proposals of the  $\pi$ -approach pathway were largely based on the electrophilicity of dihalocarbenes, observed by measuring their reactivity toward series of substituted alk-



enes.<sup>1,10,11</sup> In 1968, Hoffmann provided a theoretical rationale for the  $\pi$ -approach pathway by showing that the symmetrical cyclic  $4e^-$  transition state as in **4** was orbital-symmetry forbidden.<sup>3</sup> Using extended Hückel calculations, Hoffmann predicted a nonsymmetrical, non-least-motion approach of methylene to ethylene as in **5**, which could account for the electrophilic behavior and allow better three-center  $2e^-$  overlap.<sup>12</sup> Higher level ab initio calculations have supported the general features of the geometry **5**.<sup>4–9</sup>



In the course of computational work on the additions of  $\text{CCl}_2$ ,  $\text{CF}_2$ ,  $\text{CFOH}$ , and  $\text{C}(\text{OH})_2$  to ethylene, Rondan, Houk, and Moss pointed out the significance of a second pair of orbital interactions between the carbene HOMO and the LUMO of the alkene in the addition geometry. This is shown in the center of Chart 1, along with the more dominant carbene LUMO–alkene HOMO interactions at the left of the chart.<sup>5</sup> This interaction is responsible for the angle of carbene attack,  $\psi$ , which varies with the nucleophilicity of the carbene. This second orbital interaction also explains why the carbene approach is predicted to be so

<sup>†</sup> University of California.

<sup>‡</sup> Texas A&M University.

(1) Skell, P. S.; Garner, A. Y. *J. Am. Chem. Soc.* **1956**, *78*, 5430–5433.  
(2) Moore, W. R.; Moser, W. R.; LaPrade, J. E. *J. Org. Chem.* **1963**, *28*, 2200.

(3) Hoffmann, R. *J. Am. Chem. Soc.* **1968**, *90*, 1475–1485.

(4) Zurawski, B.; Kutzelnigg, W. *J. Am. Chem. Soc.* **1978**, *100*, 2654–2659.

(5) Rondan, N. G.; Houk, K. N.; Moss, R. A. *J. Am. Chem. Soc.* **1980**, *102*, 1770–1776.

(6) Houk, K. N.; Rondan, N. G.; Mareda, J. *J. Am. Chem. Soc.* **1984**, *106*, 4291–4293.

(7) Blake, J. F.; Wierschke, S. G.; Jorgensen, W. L. *J. Am. Chem. Soc.* **1989**, *111*, 1919–1920.

(8) Keating, A. E.; Garcia-Garibay, M. A.; Houk, K. N. *J. Am. Chem. Soc.* **1997**, *119*, 10805–10809.

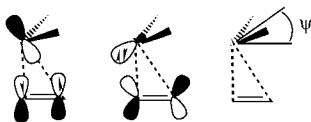
(9) Bernardi, F.; Bottoni, A.; Canepa, C.; Olivucci, M.; Robb, M. A.; Tonachini, G. *J. Org. Chem.* **1997**, *62*, 2018–2025.

(10) Doering, W. von E.; Henderson, W. A., Jr. *J. Am. Chem. Soc.* **1958**, *80*, 5274–5277.

(11) Skell, P. S.; Cholod, M. S. *J. Am. Chem. Soc.* **1969**, *91*, 7131–7137.

(12) Hoffmann, R.; Hayes, D. M.; Skell, P. S. *J. Phys. Chem.* **1972**, *76*, 664–669.

## Chart 1



asymmetric, exhibiting concerted but extremely asynchronous bond formation to the alkene carbons.

Studies at the MP2 level and results obtained using density functional theory confirm the basic asymmetric approach geometry **5**; the addition trajectory begins as an electrophilic attack but involves subsequent rotation of the carbene to achieve a final nucleophilic stage, which completes product formation.<sup>6–8</sup>

Modern methods have made it feasible to evaluate quantitatively the reaction energetics, allowing comparisons with experimental data. One obstacle to such a comparison is the difficulty of identifying a transition-state geometry along the enthalpically barrierless addition trajectory of carbenes such as  $\text{CCl}_2$  to alkenes. The location of the transition state requires the determination of the point of maximum free energy for the addition and not merely the identification of a potential energy saddle point. Houk and Rondan have pointed out that carbene cycloadditions are entropically controlled in many cases and that the position of the transition state is determined by the point at which the favorable enthalpy of the exothermic reaction compensates for the unfavorable entropy of the bimolecular addition.<sup>13</sup>

Several estimates for the barriers to carbene cycloadditions have been made computationally. In 1984, Houk and Rondan investigated the cycloadditions of  $\text{CF}_2$ ,  $\text{CCl}_2$ , and  $\text{CBr}_2$  to isobutene and tetramethylethylene. They constructed empirical model potentials for  $\Delta H$  and  $\Delta S$ , as a function of carbene–olefin separation, and assigned to  $\Delta H^\ddagger$  and  $\Delta S^\ddagger$  the values of these functions at the predicted free energy maximum. Differential activation parameters  $\Delta\Delta H^\ddagger$  and  $\Delta\Delta S^\ddagger$ , defined in this way, gave good agreement with experimental  $\Delta\Delta H^\ddagger$  and  $\Delta\Delta S^\ddagger$  values which had been reported by Giese.<sup>13</sup> In 1989, Jorgensen et al. optimized an approximate reaction trajectory for  $\text{CCl}_2$  plus ethylene and found a free energy maximum at a carbene–olefin separation of approximately 2.25 Å, corresponding to  $\Delta G^\ddagger = 11.7$  kcal/mol.<sup>7</sup> Keating et al. have more recently examined the addition of 1,2-dichloroethylidene to ethylene and to tetramethylethylene and found a free energy maximum of approximately 10.3 kcal/mol at a carbene–olefin separation of 2.7 Å for the ethylene reaction, corresponding to  $\Delta H^\ddagger = -0.5$  kcal/mol and  $\Delta S^\ddagger = -36.4$  eu.<sup>8</sup> These energies agree reasonably well with experimental activation parameters for the addition of phenylchlorocarbene to a number of alkenes determined by Turro. For these systems,  $\Delta H^\ddagger$  ranged from  $-2.3$  to  $+0.5$  kcal/mol, with  $\Delta S^\ddagger$  between  $-25.3$  and  $-23.2$  eu.<sup>14</sup>

Recent computational work using CASSCF methods gave a somewhat different picture. Bernardi et al. found singlet diradical intermediates for the addition of  $\text{CF}_2$  and  $\text{C}(\text{OH})_2$  to ethylene, with barriers of 2.7 and 0.1 kcal/mol, respectively, for cyclizations to products at the MCSCF/6-31G\* level.<sup>9</sup> These barriers disappeared when dynamic electron correlation was included, however, suggesting that the diradical character is overestimated in the CASSCF treatment. A diradical with a larger barrier to ring closure (5.7 kcal/mol) was found as an intermediate in the

(13) Houk, K. N.; Rondan, N. G. *J. Am. Chem. Soc.* **1984**, *106*, 4293–4294. Houk, K. N.; Rondan, N. G.; Mareda, J. *Tetrahedron* **1985**, *41*, 1555–1563.

(14) Turro, H. J.; Lehr, G. F.; Butcher, J. A.; Moss, R. A.; Guo, W. J. *Am. Chem. Soc.* **1982**, *104*, 1754–1756.

## Scheme 1

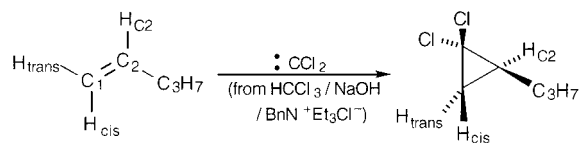


**Table 1.** Experimental KIEs ( $k_{\text{H}}/k_{\text{D}}$  or  $k^{12\text{C}}/k^{13\text{C}}$ ) for Cyclopropanations (25 °C)<sup>a</sup>

	expt 1	expt 2	expt 3
C <sub>1</sub>	1.027(2)	1.025(2)	<i>b</i>
C <sub>2</sub>	1.003(2)	1.005(2)	<i>b</i>
H <sub>trans</sub>	<i>b</i>	0.943(5)	0.950(3)
H <sub>cis</sub>	<i>b</i>	0.964(3)	0.98(1)
H <sub>C<sub>2</sub></sub>	<i>b</i>	0.986(7)	0.991(8)

<sup>a</sup> Experiments 1, 2, and 3 are reactions carried to 92.0(8), 93.4(8), and 89(1)% completion, respectively. Standard deviations are shown in parentheses. <sup>b</sup> KIEs not determined.

addition of  $\text{CF}_2$  to isobutene. This minimum probably survives the correlation correction, as evidenced by multireference MP2 single-point calculations. The studies reported here employed single-determinant density functional theory (DFT) and are susceptible to the possibility of errors resulting from the neglect of partial biradical character. These should be small for the addition of  $\text{CCl}_2$  to propene, however, both because the olefin is less sterically hindered than isobutene and because the carbene is more electrophilic and more reactive than  $\text{CF}_2$ .

Kinetic isotope effects (KIEs) are sensitive indicators of the transition-state geometry. The simultaneous measurement of  $^2\text{H}$  and  $^{13}\text{C}$  KIEs at natural abundance developed by Singleton and Thomas<sup>15</sup> has proven valuable for the study of many reaction mechanisms.<sup>16,17</sup> The successes of DFT in reproducing experiment for these cases have led us to apply the method to an investigation of the transition-state geometry for the reaction of  $\text{CCl}_2$  with propene.

## Results

The cyclopropanations of natural abundance 1-pentene on an ~3-mol scale were carried out in phase-transfer-catalyzed reactions (benzyltriethylammonium chloride) with chloroform/sodium hydroxide taken to 89–93% conversion (Scheme 1). The recovered alkene was brominated, and the resulting 1,2-dibromopentane was analyzed by  $^{13}\text{C}$  and  $^2\text{H}$  NMR and compared to a standard sample of dibromopentane derived from the original 1-pentene. The changes in  $^{13}\text{C}$  and  $^2\text{H}$  isotopic composition were calculated using the methyl group of the pentene as an “internal standard”, with the assumption that its isotopic composition does not change. From the changes in isotopic composition, the KIEs were calculated as previously described.<sup>15</sup> The results are summarized in Table 1.

The differences between the KIEs for C<sub>1</sub> and C<sub>2</sub>, and for H<sub>trans</sub>/H<sub>cis</sub> and H<sub>C<sub>2</sub></sub>, support an asymmetric transition state with greater bond formation to the terminal carbon. This rules out a carbene approach such as **4** and indicates that bond formation to the terminal carbon C<sub>1</sub> is much more advanced in the transition state. This is consistent with geometry **5**.

(15) Singleton, D. A.; Thomas, A. A. *J. Am. Chem. Soc.* **1995**, *117*, 9357–9358.

(16) DelMonte, A. J.; Haller, J.; Houk, K. N.; Sharpless, K. B.; Singleton, D. A.; Strassner, T.; Thomas, A. A. *J. Am. Chem. Soc.* **1997**, *119*, 9907–9908.

(17) (a) Beno, B. R.; Houk, K. N.; Singleton, D. A. *J. Am. Chem. Soc.* **1996**, *118*, 9984–9985. (b) Singleton, D. A.; Merrigan, S. R.; Liu, J.; Houk, K. N. *J. Am. Chem. Soc.* **1997**, *119*, 3385–3386.

To provide more quantitative conclusions, the experimental results were compared with predictions made using DFT. Geometries, energies, and normal-mode vibrational frequencies were computed along an approximate cycloaddition reaction path using the hybrid density functional method Becke3LYP,<sup>18–20</sup> with the 6-31G\* and 6-311+G\* basis sets. All electronic structure calculations were performed using the program Gaussian 94.<sup>21</sup> The reaction coordinate was defined by the distance,  $r$ , between the carbene carbon and the midpoint of the alkene double bond. This distance was constrained to values ranging from 2.0 to 3.4 Å, and the remaining degrees of freedom were fully optimized. For values of  $r$  less than 2.6 Å, normal-mode analysis revealed one imaginary frequency corresponding to the reaction coordinate.

For many values of  $r$ , we computed kinetic isotope effects using the program QUIVER.<sup>22</sup> QUIVER employs the Bigeleisen–Mayer equation to express molecular partition functions in terms of normal-mode vibrational frequencies.<sup>23</sup> Ratios of partition functions for parent and isotopically labeled species yield equilibrium isotope effects and, under the assumptions of transition-state theory, kinetic isotope effects.<sup>24,25</sup> For cycloaddition geometries with separations of 2.6 Å or more, imaginary frequencies corresponding to the reaction coordinate were either very small or nonexistent, and equilibrium isotope effects were calculated. We also used the Gaussian 94 vibrational analysis to compute entropies and free energies of reaction at 298 K along the reaction path, omitting the imaginary frequencies for such analysis where these existed. All vibrational frequencies were scaled by 0.9806, both for thermochemical analysis and for the computation of isotope effects.<sup>26</sup>

There are two possible approaches of CCl<sub>2</sub> to propene (Figures 1 and 2). In the “mode A” geometry, the carbene lone pair approaches the terminal C<sub>1</sub> carbon. The alternative “mode B” approach has more bond formation at the substituted C<sub>2</sub> carbon. The additions show initial electrophilic attack by the p orbital, followed by a rotation of the carbene for a final nucleophilic stage of reaction, in accord with expectations based on previous work.

The combination of the multisite experimental KIEs provided by this methodology with high-level theoretically predicted isotope effects was recently used to provide strong evidence for a [3 + 2] cycloaddition as the rate-determining step of the Sharpless asymmetric dihydroxylation<sup>16</sup> and has provided strong support for the DFT-predicted transition states for the Diels–Alder reaction of isoprene with maleic anhydride and epoxidation with peracids.<sup>17</sup> Consequently, KIEs calculated for mode A are pertinent for comparison with experiment. The B3LYP/6-31G\* potential surface computed for the mode A addition of

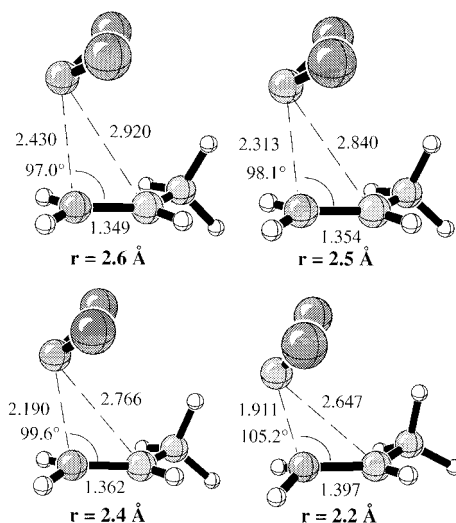


Figure 1. B3LYP/6-31G\* geometries for CCl<sub>2</sub> plus propene mode A addition at constrained values of  $r$ . Bond lengths are given in angstroms.

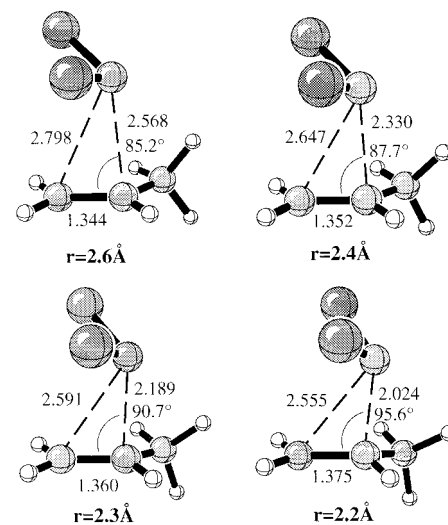


Figure 2. B3LYP/6-31G\* geometries for CCl<sub>2</sub> plus propene mode B addition at constrained values of  $r$ . Bond lengths are given in angstroms.

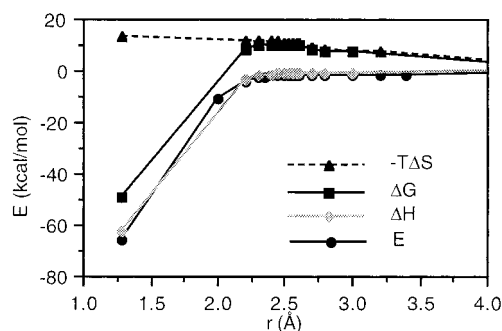


Figure 3. B3LYP/6-31G\* reaction profile for the mode A addition of CCl<sub>2</sub> to propene.  $\Delta H$ ,  $-T\Delta S$ , and  $\Delta G$  were computed at 298 K.

CCl<sub>2</sub> to propene is shown in Figure 3. There is a very shallow enthalpically stabilized complex at a carbene–olefin separation ( $r$ ) of 2.6 Å, with a barrier of less than 0.1 kcal/mol to ring formation. This complex disappears with the inclusion of the entropy of reaction, also shown in Figure 3, and the overall free energy maximum of about 10.1 kcal/mol occurs at  $r = 2.4$  Å. Single-point energy corrections to this surface at the B3LYP/cc-pVDZ<sup>27–29</sup> level make only a small difference in the reaction

(18) Lee, C.; Yang, W.; Parr, R. G. *Phys. Rev. B* **1988**, *37*, 785–789.

(19) Becke, A. D. *Phys. Rev. A* **1988**, *38*, 3098–3100.

(20) Becke, A. D. *J. Chem. Phys.* **1993**, *98*, 5648–5652.

(21) Frisch, M. J.; Trucks, G. W.; Schlegel, H. B.; Gill, P. M. W.; Johnson, B. G.; Robb, M. A.; Cheeseman, J. R.; Keith, T. A.; Petersson, G. A.; Montgomery, J. A.; Raghavachari, K.; Al-Laham, M. A.; Zakrzewski, V. G.; Ortiz, J. V.; Foresman, J. B.; Cioslowski, J.; Stefanov, B. B.; Nanayakkara, A.; Challacombe, M.; Peng, C. Y.; Ayala, P. Y.; Chen, W.; Wong, M. W.; Andres, J. L.; Replogle, E. S.; Gomperts, R.; Martin, R. L.; Fox, D. J.; Binkley, J. S.; Defrees, D. J.; Baker, J.; Stewart, J. P.; Head-Gordon, M.; Gonzalez, C.; Pople, J. A. *Gaussian 94* (Revision C.2); Gaussian, Inc.: Pittsburgh, PA, 1995.

(22) Saunders, M.; Laidig, K. E.; Wolfsberg, M. *J. Am. Chem. Soc.* **1989**, *111*, 8989–8994.

(23) Bigeleisen, J.; Mayer, M. G. *J. Chem. Phys.* **1947**, *15*, 261–267.

(24) Storer, J. W.; Raimondi, L.; Houk, K. N. *J. Am. Chem. Soc.* **1994**, *116*, 9675–9683.

(25) Olson, L. P.; Li, Y.; Houk, K. N.; Kresge, A. J.; Schaad, L. J. *J. Am. Chem. Soc.* **1995**, *117*, 2992–2997.

(26) Scott, A. P.; Radom, L. *J. Phys. Chem.* **1996**, *100*, 16502–16513.

(27) Dunning, T. H., Jr. *J. Chem. Phys.* **1989**, *90*, 1007–1023.

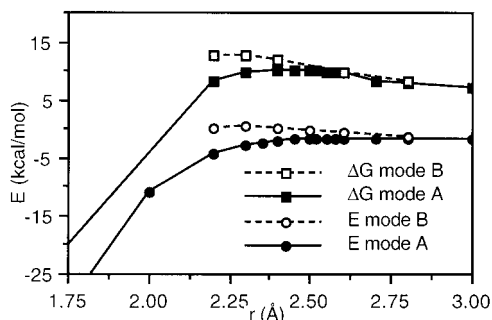


**Figure 4.** B3LYP/6-31G\* reaction profile for the mode A and B additions of CCl<sub>2</sub> to propene. ΔG was computed at 298 K.

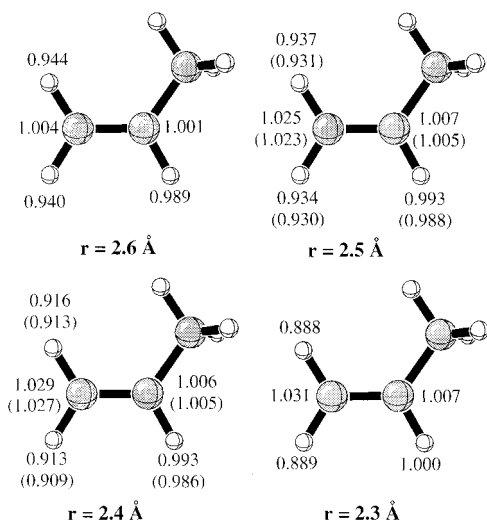


**Figure 5.** B3LYP/6-31G\* and B3LYP/6-311+G\* (in parentheses) kinetic and equilibrium ( $r = 2.6$  Å) isotope effects for the mode A addition of CCl<sub>2</sub> to propene.

profile; the free energy barrier with the corrected energies (and thermochemical analysis at the lower level) is 11.8 kcal/mol and again occurs at  $r = 2.4$  Å. The energetics of the mode B addition are compared to those of the mode A addition in Figure 4;  $\Delta G^\ddagger = 12.6$  kcal/mol at  $r = 2.3$  Å. The 2.5 kcal/mol difference in the free energy maxima for these two approaches suggests that reaction will occur almost exclusively by path A. Consequently, KIEs for mode A are used for comparison with experiment. The barrier for the addition of CCl<sub>2</sub> to ethylene is intermediate between the mode A and mode B additions to propene, with an estimated  $\Delta G^\ddagger$  of 12.2 kcal/mol at  $r = 2.4$  Å.

Kinetic or equilibrium proton and carbon isotope effects were computed for points along reaction paths A and B at the B3LYP/6-31G\* level and for several points at the B3LYP/6-311+G\* level; these are shown in Figures 5 and 6. For  $r$  values greater than 2.6 Å, equilibrium values of  $K_H/K_D$  or  $K^{12C}/K^{13C}$  are given. Figure 7 shows a plot of how the isotope effects along path A change with  $r$ . Numerical instabilities where the imaginary frequency corresponding to the reaction coordinate vanishes, at  $r = 2.6$  Å, lead to a discontinuity in the plot.

To investigate the influence of a longer alkyl chain at C<sub>2</sub>, we computed isotope effects for the addition of CCl<sub>2</sub> to 1-butene. The lowest energy conformer for this reaction trajectory has the butene in a gauche arrangement, with CCl<sub>2</sub> approaching from the opposite side of the alkene plane from the methyl group, as shown in Figure 8. In this orientation, the approach of the

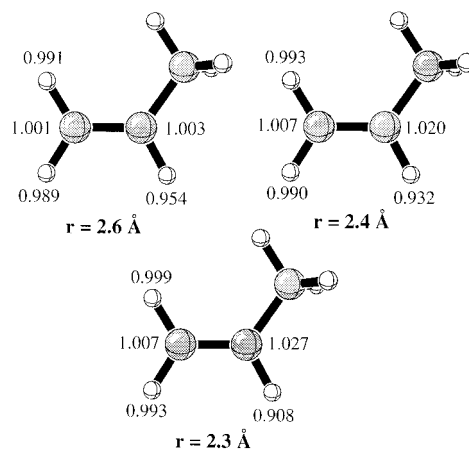


**Figure 6.** B3LYP/6-31G\* kinetic and equilibrium ( $r = 2.6$  Å) isotope effects for the mode B addition of CCl<sub>2</sub> to propene.

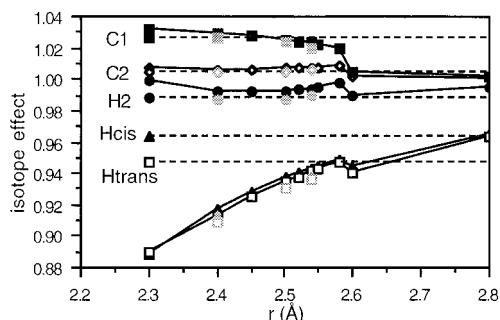


**Figure 7.** Graph of computed KIEs as a function of  $r$  compared to experiment. Experimental values are shown as dashed lines (average experimental values, except experiment 2 data for H<sub>cis</sub>). B3LYP/6-31G\* results are shown as solid black points. B3LYP/6-311+G\* results are shown as gray points.

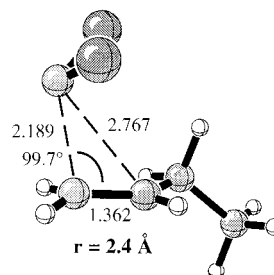


**Figure 8.** Addition of CCl<sub>2</sub> to 1-butene at  $r = 2.4$  Å.

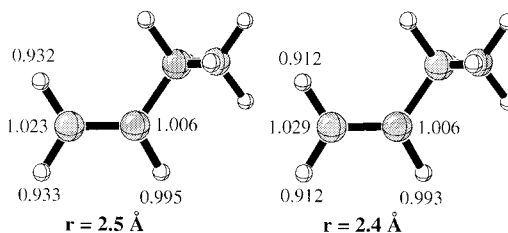


**Figure 9.** B3LYP/6-31G\*-computed KIEs for the addition of CCl<sub>2</sub> to 1-butene.

carbene to the olefin is almost identical to the geometry of the approach to propene. Isotope effects for two points along this path, with  $r = 2.4$  and 2.5 Å, are given in Figure 9. They are nearly identical to the corresponding values for propene.

## Discussion

The experimental results in Table 1 show much larger magnitude isotope effects at C<sub>1</sub> and at H<sub>cis</sub> and H<sub>trans</sub> than at C<sub>2</sub>

(28) Kendall, R. A.; Dunning, T. H., Jr.; Harrison, R. J. *J. Chem. Phys.* **1992**, *96*, 6796–6806.

(29) Woon, D. E.; Dunning, T. H., Jr. *J. Chem. Phys.* **1993**, *98*, 1358.



and  $H_{C_2}$ . Clearly, the addition is asymmetric with respect to the two alkene carbons, ruling out an approach such as **4**. The experimental isotope effects are consistent with a mode A addition, as computed to be most favorable. Partial rehybridization at  $C_1$  from  $sp^2$  to  $sp^3$  is reflected in the inverse secondary hydrogen isotope effects at  $H_{cis}$  and  $H_{trans}$ . This rehybridization is much less advanced at  $C_2$  in the transition state, revealing an asynchronicity in the formation of the two new cyclopropane C–C bonds. The normal isotope effects at the carbon centers ( $k^{12C}/k^{13C}$ ) of 1.026 ( $C_1$ ) and 1.004 ( $C_2$ ) provide further evidence for asynchronous bonding in the transition state.

Figure 7 compares experimental results to the isotope effects calculated at different values of  $r$ . If the transition state for cycloaddition lies along the chosen approximate reaction coordinate, there should be a value of  $r$  in this graph where the computed values intersect the experimental ones. The DFT prediction of the position of the free energy maximum is 2.4 Å, but a proper estimate of this value would require direct dynamics calculations.<sup>30,31</sup> Instead, we use a combination of the theory and experiment to identify an “experimental” transition state.

As shown in Figure 7, the values  $k^{12C_2}/k^{13C_2}$  and  $k_{HC_2}/k_{DC_2}$  are not very sensitive to the position of the transition state and give reasonable agreement with experiment for all values of  $r > 2.4$  Å. To assign a geometry to the experimental transition state, therefore, we focus on  $C_1$ ,  $H_{cis}$ , and  $H_{trans}$ , which show a stronger  $r$  dependence. The plot of predicted  $k^{12C_1}/k^{13C_1}$  values intersects the experimental value of about 1.026 around 2.5 Å, close to the predicted free energy maximum at 2.4 Å.  $H_{cis}$  and  $H_{trans}$ , however, match the experimental value for  $H_{trans}$  around 2.58 Å, at the B3LYP/6-31G\* level, suggesting an earlier transition state. At the B3LYP/6-311+G\* level, the isotope effects are slightly smaller for the carbon centers and slightly larger for the hydrogens, compared to the B3LYP/6-31G\* results. These values are also shown in Figure 7. At this level, the isotope effects predicted for  $C_1$ ,  $C_2$ , and  $H_{C_2}$  agree extremely well with experiment at 2.5 Å; the error for  $H_{trans}$  is approximately 0.016. While the deviation for  $H_{cis}$  is larger (0.033), the experimental error at this site is high. We conclude that the computed geometry at  $r = 2.5$  Å, shown in Figures 2 and 9 for propene and butene, are good models for the cycloaddition transition state. The free energy at 2.5 Å of 9.9 kcal/mol is only 0.1 kcal/mol lower than that at 2.4 Å, and thus is a good estimate of  $\Delta G^\ddagger$ , given the approximate nature of the reaction trajectory.

A transition state somewhat earlier than the optimal predicted value of 2.4 Å is also suggested by consideration of the experimental absolute rate for addition of  $CCl_2$  to 1-hexene. The rate of this addition in solution of  $1.1 \times 10^7 M^{-1} s^{-1}$  (21 °C) corresponds to a  $\Delta G^\ddagger$  of 7.7 kcal/mol.<sup>32</sup> This is in quite good agreement with the predicted  $\Delta G^\ddagger$  of 10.1 kcal/mol for addition to propene, but the calculational overestimation of the barrier indicates that either the calculated  $\Delta H^\ddagger$  or  $-T\Delta S^\ddagger$  (or both) is too high. With reference to Figure 3, a more steeply downward sloping enthalpy curve than that calculated would lead to an earlier transition state, and a lower  $-T\Delta S^\ddagger$  would also suggest an earlier transition state. It seems particularly plausible that the gas-phase calculations could overestimate the  $-T\Delta S^\ddagger$  for the solution reaction.

An interesting outcome of the experiments is the significantly larger  $k_H/k_D$  for  $H_{cis}$  than for  $H_{trans}$ , since there is no obvious

reason these hydrogens should be significantly different. This difference is not reproduced in the calculations. The propyl substituent on the alkene in the  $CCl_2$  plus pentene reaction is the only feature which could potentially desymmetrize  $H_{cis}$  and  $H_{trans}$ . While 1-butene is a better model for the experimental system, only a very small difference is evident between  $H_{cis}$  and  $H_{trans}$  for computed isotope effects for this reaction. We do not believe that further substitution (1-pentene vs 1-butene) would lead to a difference of more than 0.01 in  $k_{H_{cis}}/k_{D_{cis}}$  as is observed experimentally. The experimental uncertainty, which can be estimated from the differences between the experiment 2 and 3 measurements, is significant for  $H_{cis}$ , as is the standard deviation for the experiment 3 measurement. With such errors, it is possible that both  $H_{cis}$  and  $H_{trans}$  have  $k_H/k_D$  values close to that of  $H_{trans}$ . In addition, it can be discerned in previous comparisons of calculated and experimental isotope effects that  $^2H$  KIEs are calculated somewhat less accurately than  $^{13}C$  KIEs.<sup>12</sup> The reason for the greater discrepancies is unclear.

## Conclusions

Experimental kinetic isotope effects provide a sensitive indicator of the nature and location of a transition state. The isotope effects reported here for the addition of  $CCl_2$  to pentene are in good agreement with the computed reaction trajectory at the B3LYP/6-31G\* level, which favors earlier bond formation to  $C_1$  than to  $C_2$ . The carbene–alkene separation at the transition state is close to 2.5 Å. These results provide long-awaited experimental confirmation of the validity of many computational studies. After 40 years, there is definitive experimental evidence to support the mechanism of the non-least-motion carbene cycloaddition.

## Experimental Methods

**Cyclopropanations of 1-Pentene with Dichlorocarbene.** To a rapidly stirred mixture of 300 mL (192 g, 2.74 mol) of 1-pentene, 500 mL of chloroform, 2.0 g of benzyltriethylammonium chloride, 200 mL of water, and 2.65 g of benzene (NMR internal standard) held at 25 °C in a water bath was added in small portions ~400 mL of 50% aqueous NaOH over the course of 24 h. The reaction was periodically checked by GC analysis of aliquots and was stopped when  $7.6 \pm 0.8\%$  of the initial 1-pentene remained ( $93.4 \pm 0.8\%$  conversion). Approximately 1.5 L of water and 100 mL of chlorobenzene were added, and organic and aqueous phases were separated. The organic layer was then washed 3 times with 100-mL portions of brine. Simple distillation of the organic layer to afford ~50 mL of distillate followed by distillation through a 20-cm glass-bead-packed column afforded ~25 mL of low-boiling distillate. The crude 1-pentene was then brominated by the slow addition of  $Br_2$  until the  $Br_2$  color persisted. The resulting reaction mixture was fractionally distilled under a water-aspirator vacuum, and a center cut of ~5 g of 1,2-dibromopentane was collected. A standard sample of 1,2-dibromopentane was prepared by bromination of 10 mL of 1-pentene, from the same commercial lot, in an identical fashion.

Similar reactions were taken to  $92.0 \pm 0.8\%$  conversion and  $89 \pm 1\%$  conversion.

**NMR Measurements.** Neat samples of 1,2-dibromopentane at a constant 5.0 cm in height in a 10-mm NMR tube were used for  $^2H$  and  $^{13}C$  NMR measurements. A  $T_1$  determination by the inversion–recovery method was carried out for each NMR sample, and the  $T_1$  remained constant within experimental error from sample to sample.

The  $^{13}C$  spectra were obtained unlocked at 100.577 MHz on a Varian XL400 broadband NMR spectrometer, with inverse gated decoupling, calibrated  $\pi/4$  pulses, and a 120-s delays between pulses. To obtain sufficient digital resolution (5 points/ $\nu_{1/2}$  is minimal), a 158 720-point FID was zero-filled to 256K points before Fourier transformation. Integrations were determined numerically using a constant integral region set at 5 times the typical peak width at half-height for each

(30) Truhlar, D. G.; Garrett, B. C. *Acc. Chem. Res.* **1980**, *13*, 440–448.

(31) Tucker, S. C.; Truhlar, D. G. In *New Theoretical Concepts for Understanding Organic Reactions*; Bertran, J., Csizmadia, I. G., Eds.; Kluwer Academic: Dordrecht, 1989; pp 291–346.

(32) Chateaufneuf, J. E.; Johnson, R. P.; Kirchoff, M. M. *J. Am. Chem. Soc.* **1990**, *112*, 3217.

**Table 2.** Average  $^{13}\text{C}$  Integrations

completion	CHBr	CH <sub>2</sub> Br	CH <sub>3</sub>	<i>n</i>
92.0(8)%	1097(4)	1166(3)	1000	8
standard	1087(4)	1091(3)	1000	8
<i>R/R</i> <sub>0</sub>	1.008	1.069		
93.4(8)%	1012(4)	1027(4)	1000	8
standard	1026(4)	1098(3)	1000	8
<i>R/R</i> <sub>0</sub>	1.014	1.069		

peak. A zeroth-order baseline correction was generally applied, but in no case was a first-order (tilt) correction applied.

$^1\text{H}$ -decoupled  $^2\text{H}$  spectra were obtained unlocked at 61.395 MHz on a Varian XL400 spectrometer equipped with a broadband probe. A 2.276-s delay was used between calibrated  $\pi/4$  pulses. A data set of 2K points was collected and zero-filled to 64K. The tuning of each sample was carefully optimized on the basis of the peak shape for the methyl group.

$^{13}\text{C}$  measurements were carried out for the reactions taken to 92.0 and 93.4% conversion. The integration of the methyl group carbon in each spectrum was set at 1000. The average integrations for the other carbons for each reaction, along with the standard results for the starting materials, are shown in Table 2, along with the standard deviation of the observed values in parentheses. In each case, *n* is the total number of spectra obtained. Table 2 also shows the values for *R/R*<sub>0</sub>, calculated as the ratio of average integrations for recovered material relative to the standard. The standard deviations were calculated from the following formula:

$$\Delta R/R_0 = R/R_0((\Delta \text{IntSample}/\text{IntSample})^2 + (\Delta \text{IntStandard}/\text{IntStandard})^2)^{1/2} \quad (1)$$

The KIEs listed in Table 1 were then calculated from eq 2, with the standard deviations calculated from eqs 3–5. All of these equations are taken from ref 15, its Supporting Information, and references therein.

$$\text{KIE}_{\text{calcd}} = \frac{\ln(1-F)}{\ln[(1-F)R/R_0]} \quad (2)$$

$$\Delta \text{KIE}_F = \frac{\partial \text{KIE}}{\partial F} \Delta F = \frac{-\ln(R/R_0)}{(1-F) \ln^2[(1-F)R/R_0]} \Delta F \quad (3)$$

$$\Delta \text{KIE}_R = \frac{\partial \text{KIE}}{\partial (R/R_0)} \Delta (R/R_0) = \frac{-\ln(1-F)}{(R/R_0) \ln^2[(1-F)R/R_0]} \Delta (R/R_0) \quad (4)$$

$$\Delta \text{KIE} = \text{KIE}((\Delta \text{KIE}_R/\text{KIE})^2 + (\Delta \text{KIE}_F/\text{KIE})^2)^{1/2} \quad (5)$$

The  $^2\text{H}$  KIEs were determined in a similar fashion for the reactions taken to 93.4 and 89% conversion.

**Acknowledgment.** We thank the National Science Foundation and the Robert A. Welch Foundation for financial support of this research and the National Center for Supercomputing Applications at the University of Illinois at Urbana–Champaign and the Office of Academic Computing at UCLA for computing resources. D.A.S and S.R.M thank NIH Grant No. GM-45617 for financial support. A.E.K. acknowledges the NSF for a graduate research fellowship.

JA981427X